Cr (III), Mn (II), Co (II), and Ni (II) complexes with a bidentate Mannich base: Synthesis, bioevaluation, and docking studies of the free ligand

Marwa Jassim Al-Muhamadawi*, Rehab Abdul Mahdi Al-Hassani

ORIGINAL RESEARCH ARTICLE

Department of Chemistry, College of Science, Mustansiriyah University, Baghdad, 10045, Iraq

*Corresponding author: Marwa Jassim Al-Muhamadawi, marwajassim313@uomustansiriyah.edu.iq

ARTICLE INFO

Received: 14 September 2025 Accepted: 30 September 2025 Available online: 22 October 2025

COPYRIGHT

Copyright © 2025 by author(s). Applied Chemical Engineering is published by Arts and Science Press Pte. Ltd. This work is licensed under the Creative Commons Attribution-NonCommercial 4.0 International License (CC BY 4.0).

https://creative commons.org/licenses/by/4.0/

ABSTRACT

The design and synthesis of novel coordination compounds have attracted considerable interest in the field of inorganic chemistry field, particularly as a result of Mannich base ligands' capability of forming stable complexes with metal ions often result in an enhancement of the chemical and physical characteristics. In the present study, a new Mannich base ligand was synthesized by condensing benzaldehyde, di-benzylamine, and 5-chloro-2mercapto-oxazole. The ligand has been thoroughly characterized using elemental analysis (CHNS), Fourier-transform infrared spectroscopy (FTIR), ultraviolet-visible spectroscopy (UV-Vis), proton and carbon nuclear magnetic resonance spectroscopy (1H NMR and 13C NMR), and mass spectrometry. As a result, the ligand's coordination complexes with ions of Co (II), Cr (III), Mn (II), and Ni (II) had been synthesized and characterized through FT-IR, magnetic susceptibility measurements, UV-Vis spectroscopy, molar conductivity, and elemental analyses for the purpose of elucidating their electronic and structural features. FTIR spectra had confirmed the ligand's bidentate coordination mode across all metal complexes. The electronic spectra and magnetic moment data indicated that the resulting complexes are of a variety of geometries according to the center of the metal. Molar conductivity measures have revealed that all complexes exhibited nonelectrolytic behavior in the solutions suggesting high structural integrity and stability level. In addition to that, molecular docking studies were performed on the free ligand using the gold program to evaluate its possible interactions with the targeted enzyme's active site. The docking analyses showed that ligand has the ability to effectively interact with residues of key amino acids within the enzyme's active site, which results in the formation of stable binding conformations in addition to extensive bonding of hydrogen bonds, which support its possible biological activities. Additionally, the biological activities of the synthesized ligand and the biological activities of its metal complexes were assessed in vitro against bacterial strains, which include Escherichia coli and Staphylococcus aureus, in addition to some fungal species, like Penicillium spp. and Aspergillus flavus. The MICs (i.e., minimum inhibitory concentrations) were determined to assess the compounds' anti-microbial potency. Standard antibiotics, Fluconazole and Ampicillin, have been used as reference drugs. Results showed that metal complexes exhibited an improved anti-microbial activity compared with the reference drugs and free ligands, which has highlighted their potential for a wider range of pharmaceutical applications.

Keywords: 5-chloro-2-mercapto-oxazole; benzaldehyde; mannich base ligand; mannich base complexes; coordination complexes; FTIR; UV-Vis spectroscopy; transition metals; molecular docking

1. Introduction

The broad range of Mannich base ligand applications, in addition to their complexes, drew much attention. In the field of medicine, commonly, they're utilized as potential pharmacological agents. When utilized as agents of complexation, they result in greatly enhancing the biological activities of complexes that have been created by them^[1]. Mannich reaction is a process of condensation involving 3 components, which are molecules that have active hydrogen (an acidic hydrogen atom), an aldehyde, and a secondary or a primary amine^[2]. The actual reaction represents one of the powerful tools in organic chemistry, providing is an efficient and straightforward way for generating C-N bonds. The Mannich bases represent highly adaptable molecules, these molecules can be modified for the purpose of adding various functional groups, leading to a vast array of compounds that have a set of distinctive properties^[2]. Mannich bases, as well as their derivatives significantly impact the variety of the chemical applications and were viewed as crucial to pharmaceutical sciences. This research showed that they have been effective in a broad range of areas, which include the antifungal, antitubercular, antiviral, anti-mycobacterial, antitumor, anti-HIV, anticancer, and cytotoxic activities. Additionally, the basic Mannich sidechain showed some particular characteristics, like antiinflammatory, analgesic, anti-malarial, and antibacterial characteristics. Strong antibacterial, antiviral and anticancer effects were also demonstrated by the Mannich base ligands combined with transition metals, which had underscored their significance in researching the transition metal and drug development^[3]. Those substances have played the base ligand and antioxidant role and showed effectiveness in the decrease of base ligands. Mannich reaction represents one of the efficient and fundamental methods in modern chemical synthesis, which is essential for producing crucial bio molecules such as lactams, peptides, amino acids, and amino alcohols, amongst other biologically important substances^[2,3]. This reaction has been considered highly valuable in the chemistry field, due to the fact that it shows its versatility and practicality at the formation of some significant chemical bonds. Various chemical and biological applications are supported by molecules that are produced by that reaction, also functioning as adaptable intermediates^[4-9]. A crucial nucleophilic addition method for the formation of carbon-carbon bonds, the Mannich reaction is essential to chemical synthesis of a broad range of medications and natural compounds. Due to the fact that they're capable of creating stable coordination complexes with various transition metal ions, which have their therapeutic properties, Mannich bases are especially significant in medicinal chemistry. These bases are essential building blocks for producing many naturally occurring physiologically active compounds and serve as intermediates in drug design. Because of the special coordination characteristics of these ligands with various metal ions, there has been an increase in interest recently in the synthesis and biological assessment of Mannich base derivatives and their metal complexes^[10,11]. This study aims to synthesize a novel Mannich base derived from benzaldehyde, dibenzylamine, and 5-chloro-2-mercapto-oxazole, and to investigate its spectroscopic properties. In addition, coordination complexes of this base will be prepared with transition metal ions like Cr (III), Mn (II), Co (II), and Ni (II), and their structures and electronic characteristics will be analyzed. This work provides a unique contribution through the design and synthesis of a Mannich base incorporating the 5-chloro-2-mercapto-oxazole moiety, which has not been extensively explored in coordination chemistry. By examining the behavior of this ligand in forming complexes with various metal ions, the study seeks to enhance understanding of the correlation between molecular structure and physicochemical characteristics in such systems.

2. Materials and methods

2.1. Synthesis of mannich base

The Mannich base ligand has been synthesized following a reported protocol^[12], utilizing equimolar amounts of 5-chloro-2-mercapto-oxazole (1g), benzaldehyde (1.2g), and di-benzylamine (1.2g), all dissolved in ethanol. The reaction has been carried out in a (75mL) glass beaker under continuous stirring at ambient temperature while maintaining ice-cold conditions for (2hr to 4hrs). Reaction progress has been monitored by thin-layer chromatography (TLC). Upon completion, the mix has been left to stand overnight at a low temperature to facilitate crystallization. This formed solid has been collected by vacuum filtrations, washed with the use of cold ethanol (10.0mL), and purified through recrystallization using hot ethanol. The final product was air-dried at room temperature and kept in a desiccator. The reactions afforded the target Mannich base with a yield of approximately 95%. The overall synthetic pathway is presented in (**Figure 1**).

Figure 1. Synthetic pathway.

2.2. Synthesis of metal complexes (CrL1, MnL1, CoL1, and NiL1)

A hot ligand ethanolic solution (0.25g, 0.00053mole) was gradually mixed with a hot ethanolic solution of metal chloride of MnCl₂·4H₂O, CrCl₃·6H₂O, NiCl₂·6H₂O, and CoCl₂·6H₂O under reflux conditions and while stirring continuously. (0.104, 0.141, 0.125, and 0.126) grams. The mixture was chilled and kept in the refrigerator for a few hours after refluxing for one to two hours at 25°C. Each case-colored solid complex was separated, filtered, washed with 50% alcohol, and then allowed to dry. Table 1 lists the complexes and the physicochemical characteristics of the generated ligand.

2.3. In silico molecular docking studies

Nepetin's molecular structure was initially constructed using ChemDraw Professional (version 16.0). Subsequently, molecular energy minimization was performed utilizing the licensed CCDC genetic algorithm embedded within the GOLD software suite (Hermes 2021.2.0, Build 327809). This platform has been employed to conduct molecular docking research for the prepared compounds, enabling visualization and analysis of protein–ligand interactions, including hydrogen bonding, close contact points, and bond length calculations. The crystal structure of Cyclin-Dependent Kinase 2 (CDK2) (PDB ID:1hck) had been obtained from the Protein Data Bank. Before docking, non-essential receptor molecules have been removed, and polar hydrogen atoms have been added to water molecules. All docking simulations were executed using the GOLD software under the Windows 10.0 Professional operating system^[13].

3. Results and discussions

3.1. Characterization of the ligand and its metal complexes

The suggested molecular formulae for the synthesized Mannich base ligand (L) and its corresponding metal complexes CrL, MnL, CoL, and NiL are consistent with the observed physical characteristics and elemental analytical data, as presented in (**Table 1**). Based on the general formulations [CrL₂(H₂O)Cl₃], [MnL₂Cl₂(H₂O)₂], [CoL₂Cl₂]·C₂H₅OH, and [NiL₂(C₂H₅OH)₂Cl₂], experimental results suggest that metal-The

to-ligand stoichiometric ratio in all complexes is 1:1. The synthesized complexes exhibited good solubility in many different organic solvents and demonstrated stability under ambient atmospheric conditions. The free ligand purity has been confirmed via TLC. Furthermore, elemental analysis (CHNS) results for hydrogen, nitrogen, carbon, sulfur, and the respective metal ions were found to be in close agreement with theoretical values, thereby validating the proposed molecular structures of the ligand and its metal complexes.

Table 1. Analytical and Physical data of ligand L₁ as well as its complexes.

Comp sym.	Experimental Formula	MP°C	Colour	Expe	Metal content			
	M.wt (g/mol)			C%	Н%	N%	S%	found (calc.)%
L_1	C28H23Cl N2OS 470.8g/mole	138-140	Light brown	71.5 (65.54)	4.89 (4.82)	5.96 (7.01)	10.50 (10.79)	
CrL_1	[Cr (C ₂₈ H ₂₅ Cl N ₂ O ₂ S) Cl ₃] 647.28 g/mole	355d	Dark green	52.04 (51.95)	5.21 (4.94)	4.44 (4.32)	3.97 (3.86)	52.04 (51.95)
MnL_1	[Mn (C ₂₈ H ₂₇ Cl N ₂ O ₃ S) Cl ₂] 632.66 g/mole	318d	Light pink	53.21 (53.15)	5.12 (5.05)	4.60 (4.42)	4.38 (4.26)	53.21 (53.15)
CoL_1	[Co (C ₂₈ H ₂₃ Cl N ₂ OS) Cl ₂] 600.72 g/mole	328d	Blush green	56.05 (55.97)	5.48 (5.32)	4.80 (4.66)	3.95 (3.82)	56.05 (55.97)
NiL_1	[Ni (C ₃₂ H ₃₅ Cl N ₂ O ₃ S) Cl ₂] 692.54 g/mole	320d	Light green	55.64 (55.49)	4.88 (4.62)	4.19 (4.04)	5.11 (5.05)	55.64 (55.49)

d=Decomposed

3.2. IR spectroscopy

FT-IR spectrum of free ligand (L₁) had shown characteristic absorption bands at 1076, 1216, 1257, and 1321 cm⁻¹, which are a result of the stretching vibrations of the N–C=S group. Additional bands observed at 823 and 860 cm⁻¹ correspond to the C=S stretching vibrations, while the absorptions at 2722, 2795, and 2912 cm⁻¹ are associated with the stretching modes of the ph–CH–N moiety. These assignments are consistent with previously reported data^[14] and are summarized in (**Table 2**). Upon complexation with metal ions, significant shifts and intensity changes have been observed in the IR spectra of the resulting metal complexes when compared to the free ligand. These variations provide strong evidence for coordination through specific donor atoms in the ligand framework.

A. In the metal complexes, the v(C=S) stretching band of the ligand had exhibited a noticeable shift to lower wavenumbers, appearing at 823 and 860 cm^{-1[15]}. This downward shift is an indication of the involvement of the sulfur atom of the thio-carbonyl group in coordination with the metal ion. Moreover, The shift suggests a degree of π -electron delocalization between the metal center and the ligand, further supporting the formation of a metal-ligand coordination bond through sulfur donor site^[15–16].

B. In the free ligand's FTIR spectrum, v(N-C=S) stretching vibrations appeared at 1076, 1216, 1257, and 1321 cm⁻¹. Upon the complexation, those bands had shifted to lower frequencies, which are accompanied by a noticeable decrease in the degree of intensity and the changes in the band shape. These spectral alterations are considered reliable indicators of coordination between metal ions and both nitrogen and sulfur atoms of the thio-carbonyl moiety^[15–17]. Such coordination supports the proposed bidentate binding mode of the ligand in the formation of stable metal complexes.

C. The v(ph–CH–N) stretching vibrations of the aminomethyl group in Mannich base ligand were observed at 2722, 2795, and 2912 cm⁻¹. In the metal complex spectra, those bands were shifted to lower wavenumbers, which indicates nitrogen atom involvement from the dibenzyl amine moiety in coordination with the central metal ion^[16,17]. This shift further supports the proposed coordination mode, highlighting the role of the nitrogen donor site in complex formation.

- **D.** The FTIR spectra of metal complexes of ligand (L_1) exhibited new bands of absorption that had not been present in the free ligand spectrum. Those newly observed bands were a result of stretching vibrations of v(M-S), v(M-N), and v(M-Cl), respectively [18-21]. The appearance of these bands provides strong evidence for the coordination of the ligand with metal ions through the aminomethyl group's nitrogen atom and the thiocarbonyl group's sulfur atom. This confirms the bidentate nature of the ligand (L_1), coordinating through both donor sites with all metal ions that have been examined.
- **E.** Water absorption bands indicative of inner-sphere coordination had been observed in the spectra of CrL₁ and MnL₁ complexes at 3040cm⁻¹ and 3440 cm⁻¹, respectively. These bands suggest that there are coordinated water molecules that are bonded directly to metal centers, further supporting the proposed structural formulations of these complexes^[18,19].
- **F.** In the NiL₁ complexes, the presence of coordinated ethanol was confirmed by the appearance of broad stretching bands in a 3545–3392cm⁻¹ range, corresponding to O–H vibrations^[19].
- **G.** The spectra of CrL_1 , MnL_1 , and NiL_1 complexes have shown a new weak band at frequency (510cm⁻¹) that was a result of the (M-O) stretching frequency^[18–21].

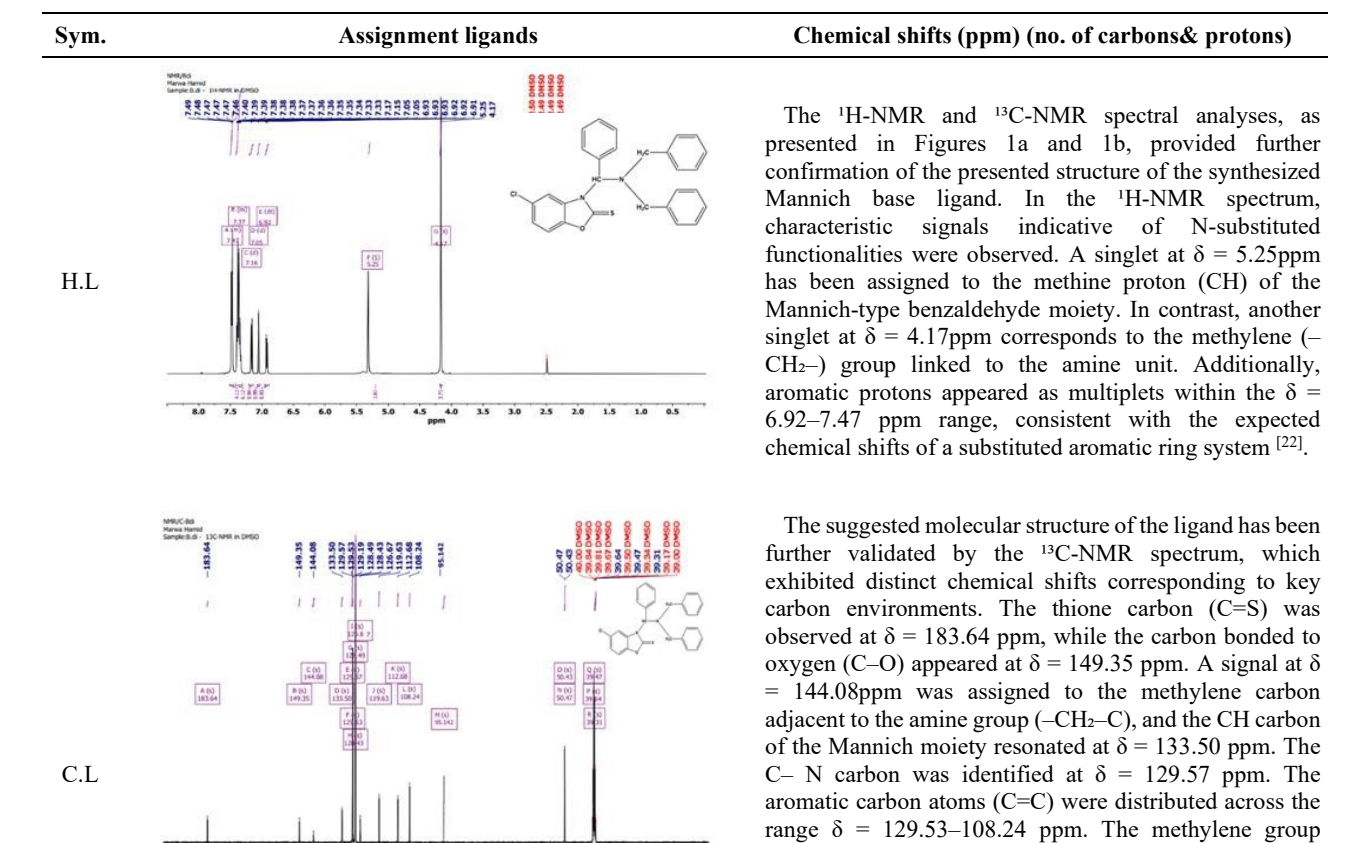
Table 2. Infrared spectral data of (Cm⁻¹) ligand (L₁) and its metal complexes.

Comp.	υ(C=S)	υ(N-C=S)	υ(ph-CH-N)	υ(M-N)	v(M-S)	υ(M-Cl)	υ(M-O)	Nots.
Lı	823 860	1076 1216 1257 1321	2722 2795 2912					
CrL_1	803 848	1029 1211 1262	2785	492	475	402	506	Rocking 3040 H ₂ O
MnL_1	802 847	1051 1199 1259	2784	511	472	405	512	Rocking vOHof H ₂ O 3440
CoL_1	824 849	1062 1149 1230 1262	2786 2903	536	485	403		
NiL ₁	804 849	1062 1092 1220 1260	2917	488	460	405	511	υΟΗ(ethanol) 3395 3499

3.3. NMR Spectroscopy

The proposed structure of the synthesized ligand was confirmed by both ¹H-NMR and ¹³C-NMR spectroscopy, showing characteristic signals for key functional groups as presented in (**Table 3**).

Table 3. ¹H and ¹³C NMR spectral data of the synthesized free ligand



3.4. Mass spectrometry

The molecular structure of the synthesized ligand has been further confirmed by mass spectrometric analysis. The mass spectrum (**Figure 2**) displayed a prominent molecular ion peak at m/z = 469.10, corresponding 164 to the molecular ion with loss of a hydrogen atom (M^+ –H). This observation provides additional 165 confirmation of the successful synthesis of the Mannich base ligand.

(CH₂) of the amine moiety appeared in the region of δ = 50.47–50.43 ppm, while the CH group of the Mannich center was detected at δ = 95.14 ppm. Signals corresponding to the DMSO-d₆ solvent were observed at δ = 39.64 and 39.31 ppm. These comprehensive ¹³C-NMR data provide strong evidence for the successful synthesis and structural integrity of the Mannich base ligand^[23].

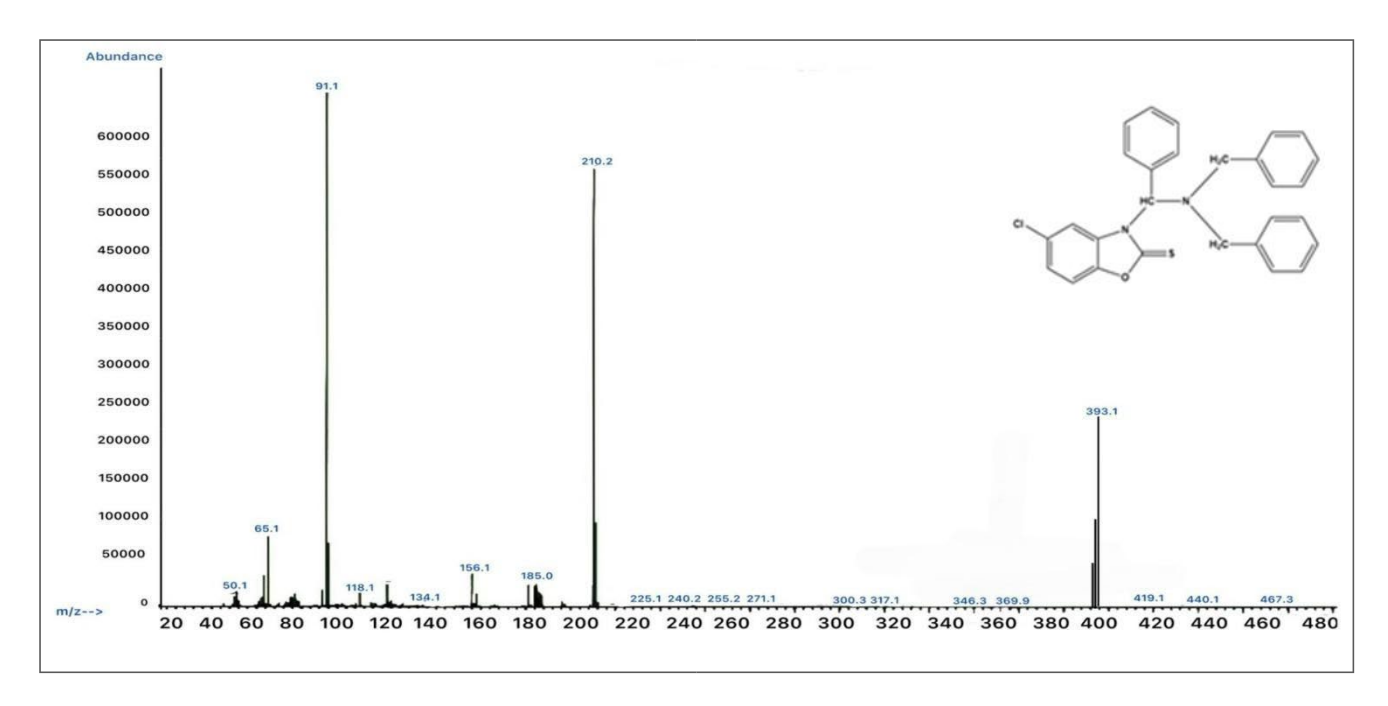
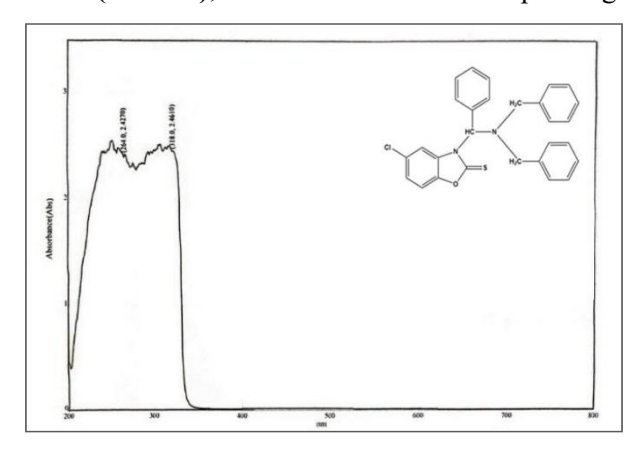


Figure 2. Mass spectrum of the ligand.

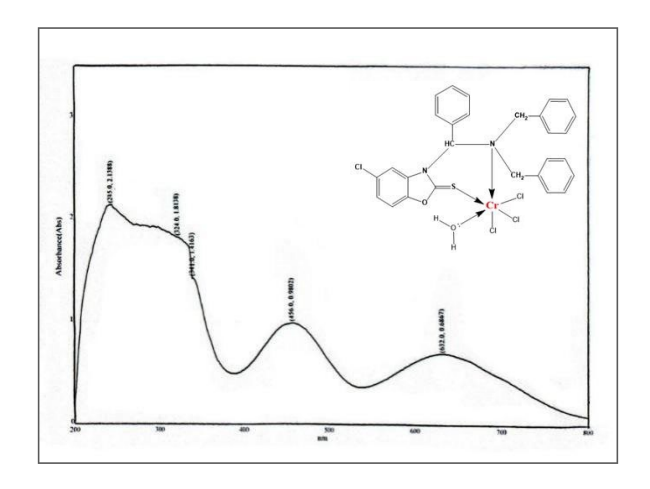
3.5. Electronic absorption, Conductivity, and Magnetic susceptibility

Two bands of absorption at (264nm, 37878cm-1) and (318nm, 31446cm⁻¹) in the ligand (L) (U.V.-Vis) spectra in absolute ethanol have been a result of $(\pi \to \pi^*)$ and $(n \to \pi^*)$ intra-ligand transitions^[24]. A new band appears in the visible and ultraviolet spectra when (L₁) complexes with metal ions. These bands were ascribed to ligand field transitions and M-L charge transfer. Bands of maximum absorption of complexes in the chloroform have been described in (**Table 4**), in addition to their corresponding assignments.



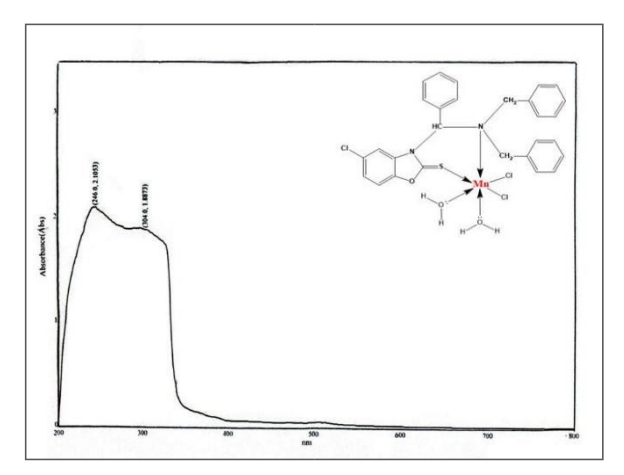
\triangleright Cr complexes of L₁

Three bands of absorption for Cr(III) complex have been observed at 15822, 21929, and 29325cm⁻¹, which are an indication of octahedral geometry around the chromium center. These bands are attributed to the following electronic transitions: ${}^{4}A_{2}g(F) \rightarrow {}^{4}T_{1}g(F)$ (v_{1}), ${}^{4}A_{2}g(F) \rightarrow {}^{4}T_{2}g(F)$ (v_{2}), and ${}^{4}A_{2}g(F) \rightarrow {}^{4}T_{1}g(P)$ (v_{3}), respectively^[24,25]. The calculated ratio of (v_{2}/v_{1}) is 1.39, which closely aligns with the typical value for octahedral Cr(III) complexes, supporting the proposed geometry^[24,25]. The magnetic moment of the solid complex is 3.82 Bohr Magnetons (BM), consistent with the presence of 3 unpaired electrons. Furthermore, the measurement of molar conductivity in DMF confirmed the non-electrolytic nature, indicating that it behaves as a neutral species in solution^[25,26] (**Table 4**), Structural Geometry (**Figure 3**).



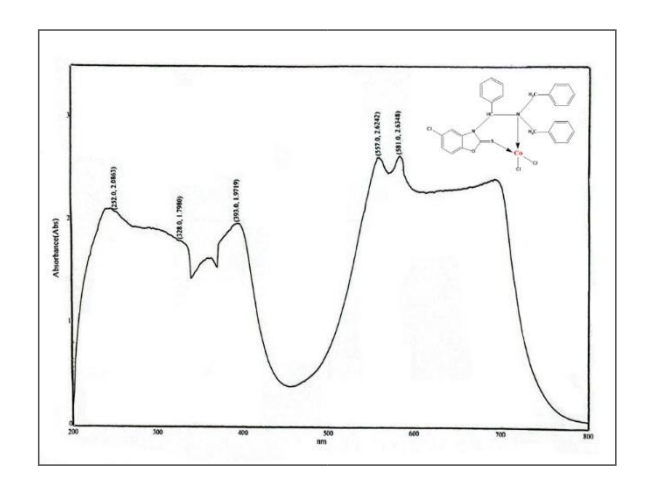
Mn complex of L₁

The octahedral geometry of the Mn (II) complex was confirmed by the presence of weak absorption bands in the UV-Vis spectrum at 19607, 25641, and 28169 cm⁻¹. Those bands are assigned to spin forbidden transitions: ${}^6A_1g \rightarrow {}^4T_1g({}^4G)$ (v_1), ${}^6A_1g \rightarrow {}^4Eg({}^4G)$ (v_2), and ${}^6A_1g \rightarrow {}^4Eg({}^4D)$ (v_3), respectively^[27-29]. The measurement of molar conductivity in DMF had indicated that the complex behaves as a non-electrolyte, suggesting it remains neutral in solution. Additionally, the magnetic moment value is 5.22 Bohr Magnetons (BM), which is consistent with a high-spin d⁵ Mn (II) ion in an octa-hedral environment (**Table 4**), Structural Geometry (**Figure 3**).



➤ Co complex of L₁

The value of magnetic moment of 4.72 Bohr Magnetons (BM) for Co(II) complex suggests a high-spin configuration. The electronic absorption spectrum recorded in chloroform revealed three distinct bands: at 680nm (14705 cm⁻¹), assigned to ${}^4A_2 \rightarrow {}^4T_2(F)$ (v_1) transition; at 581 nm (17211 cm⁻¹), corresponding to the ${}^4A_2 \rightarrow {}^4T_1(F)$ (v_2) transition; and at 557 nm (17953 cm⁻¹), attributed to the ${}^4A_2 \rightarrow {}^4T_1(P)$ (v_3) transition[²⁸]. Ligand field parameters, including the crystal field splitting energy (10Dq =14720cm⁻¹) and Racah parameter (B=566cm⁻¹), were estimated using the Tanabe–Sugano diagram for a d⁷ electronic configuration, indicating that the complex adopts a tetrahedral geometry[^{24,25,30}]. Nephelauxetic ratio (β) has been calculated to be 0.533, reflecting a high covalency degree in metal-ligand bonding. Furthermore, molar conductivity measurements confirmed the non-electrolytic nature of the complex in solution, as presented in (**Table 4**) and Structural Geometry (**Figure 3**).



➤ Ni complex of L₁

The Ni(II) complex's electronic spectrum in chloroform (CHCl₃) revealed four absorption bands at 791nm (12642 cm⁻¹), 683 nm (14641 cm⁻¹), 522 nm (19157 cm⁻¹), and 411 nm (24330 cm⁻¹), corresponding to the transitions: ${}^{3}\text{A2g} \rightarrow {}^{3}\text{T2g}(F)$ (v₁), ${}^{3}\text{A2g} \rightarrow {}^{3}\text{T1g}(F)$ (v₂), ${}^{3}\text{A2g} \rightarrow {}^{3}\text{T1g}(P)$ (v₃), and a charge transfer transition (L \rightarrow Ni) (v₄)^[29], respectively^[29] (**Table 4**). Based on the Tanabe–Sugano diagram for a d⁸ electronic configuration, ligand field parameters were calculated: 10 Dq = 11389 cm⁻¹, Racah parameter B' = 515 cm⁻¹, and nephelauxetic ratio β = 0.58. The relatively low β value indicates a significant degree of covalency in the metalligand bonding. Additionally, the v₂/v₁ ratio was found to be 1.16, which, along with the other spectral data supports the presence of octa-hedral geometry around Ni (II) ion. The magnetic moment of the complex was measured at 2.80 Bohr Magnetons (BM), which falls within the typical range (2.80–3.50BM) for octahedral Ni (II) complexes, further confirming the proposed geometry (**Table 4**)^[31]. Molar conductivity measurements showed that the complex behaves as a non-electrolyte in solution. These findings, in conjunction with elemental analysis (CHNS), FTIR spectroscopy, and flame atomic absorption results, strongly support an octahedral geometry around the Ni (II) center^[25,30] (**Table 4**), Structural Geometry (**Figure 3**).

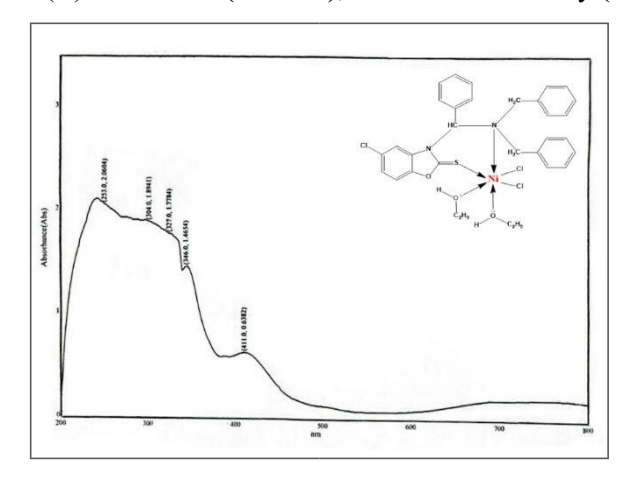


Table 4. Electronic spectrum, Magnetic moment (BM) and Conductance in (DMF) for (L₁) complexes.

No.	$\begin{array}{c} \textbf{Maximum absorption} \\ \upsilon_{max}(\textbf{cm}^{-1}) \end{array}$	* Rand assignment		μeff. B.M	Proposed geometry
L_1	31446 37878	$\begin{array}{c} \pi{\rightarrow}\pi^* \\ n{\rightarrow}\pi^* \end{array}$			
CrL ₁	15822 21929 29325	${}^{4}A_{2}g(F) \rightarrow {}^{4}T_{1}g(F)(v_{1})$ ${}^{4}A_{2}g(F) \rightarrow {}^{4}T_{2}g(F)(v_{2})$ ${}^{4}A_{2}g(F) \rightarrow {}^{4}T_{1}g(F)(v_{3})$	10.22	3.82	O.h
MnL_1	19607 25642 28169	${}^{6}A_{1}g \rightarrow {}^{4}T_{1}g({}^{4}G)(v_{1})$ ${}^{6}A_{1}g \rightarrow {}^{4}Eg({}^{4}G)(v_{2})$ ${}^{6}A_{1}g \rightarrow {}^{4}Eg({}^{4}D)(v_{3})$	19.88	5.22	O.h

CoL ₁	14705 17211 17953	$^{4}A_{2} \rightarrow ^{4}T_{2(F)}(v_{1})$ $^{4}A_{2} \rightarrow ^{4}T_{1(F)}(v_{2})$ $^{4}A_{2} \rightarrow ^{4}T_{1(P)}(v_{3})$	15.43	4.72	T.h
NiL_1	12642 14641 19157 24330	${}^{3}A_{2}g \rightarrow {}^{3}T_{2}g (F)(v_{1})$ ${}^{3}A_{2}g \rightarrow {}^{3}T_{1}g(F)(v_{2})$ ${}^{3}A_{2}g \rightarrow {}^{3}T_{1}g(P)(v_{3})$ $L \rightarrow M (C.T)$	10.39	2.78	O.h

Table 4. (Continued)

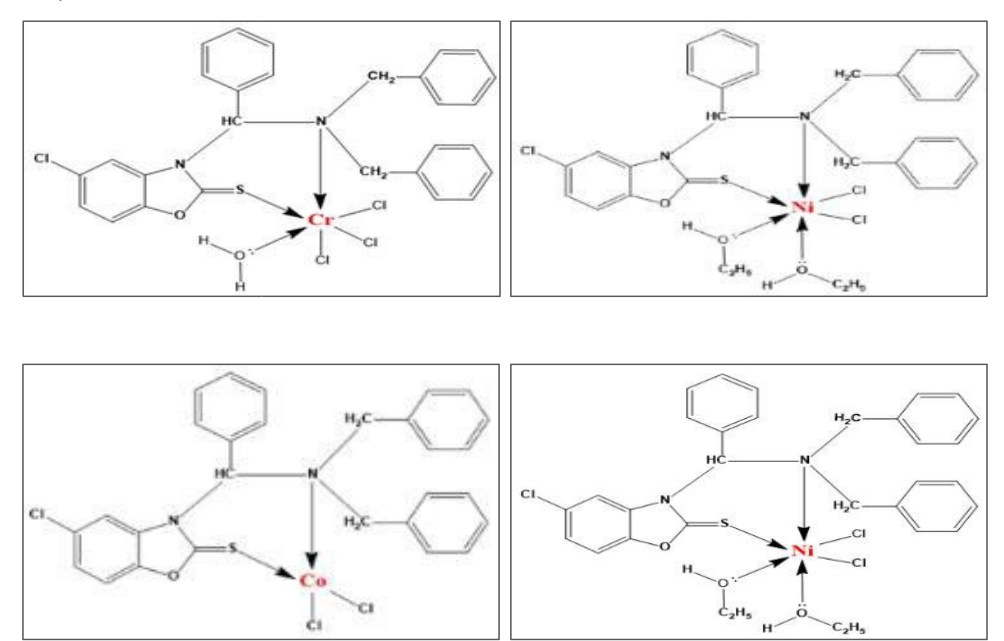


Figure 3. The Proposed Structural Geometry of Resulting Complexes.

3.6. Antibacterial and antifungal activity

The literature indicates that certain heterocyclic compounds, particularly oxazole ring derivatives, possess a broad spectrum of pharmacological activities, with notable antibacterial and antifungal properties. These characteristics render them promising candidates for developing new antimicrobial agents^[32,33]. The antibacterial and anti-fungal activities of synthesized Mannich base ligand (L) and its corresponding metal complexes have been presented in (Table 5). Inhibition zone diameters were measured in millimeters to assess their efficacy. The antimicrobial potential of synthesized compounds has been evaluated against selected grampositive (S. aureus) and gram-negative (E. coli) bacterial strains, in addition to fungal strains (Aspergillus flavus and Penicillium spp.), using various concentrations. Ampicillin and fluconazole have been 246 employed as standard reference drugs for antibacterial and antifungal comparisons, respectively, as shown in 247 (Table 5). Dimethyl sulfoxide (DMSO) was utilized as a solvent control in all assays. Results have revealed that 248 both the free ligand and its metal complexes demonstrated higher anti-bacterial activity than the reference 249 drug, except for MnL complex. Notably, the CrL, CoL, and NiL complexes exhibited the most potent inhibitory effects against both bacterial strains. Similarly, the antifungal activity of the ligand and its metal complexes exceeded that of fluconazole^[34], except for MnL, which displayed comparatively weaker inhibition, as detailed in (Table 5).

Table 5. MIC for free ligand and their metal complexes.

Comp.	Staphylococcus aureus Escherichi									nerichia	coli					
	0.025	0.05	0.1	0.25	0.5	1	2.5	5	0.025	0.05	0.1	0.25	0.5	1	2.5	5
DMSO	-	-	-	-	-	-	-	-	-	-	-	-	-	-	-	-
L_1	+	+	+	MIC	-	-	-	-	+	+	MIC	-	-	-	-	-
$[CrL_1]$	+	+	MIC	-	-	-	-	-	+	MIC	-	-	-	-	-	-
$[MnL_1]$	+	+	+	+	+	+	MIC	-	+	+	+	+	+	-	MIC	-

[CoL ₁]	+	+	MIC	-	-	-	-	-	+	+	+	MIC	-	-	-	-
$[NiL_1]$	+	+	MIC	-	-	-	-	-	+	MIC	-	-	-	-	-	-
Ampicillin	+	+	+	+	MIC	-	-	-	+	+	+	+	MIC	-	-	-
Comp.		Aspergillus flavus								Penicillium spp.						
	0.025	0.05	0.1	0.25	0.5	1	2.5	5	0.025	0.05	0.1	0.25	0.5	1	2.5	5
DMSO	-	-	-	-	-	-	-	-	-	-	-	-	-	-	-	-
L_1	+	MIC	-	-	-	-	-	-	+	+	MIC	-	-	-	-	-
$[CrL_1]$	+	+	MIC	-	-	-	-	-	+	+	+	MIC	-	-	-	-
$[MnL_1]$	+	+	+	+	+	MIC			+	+	+	+	+	+	MIC	-
$[CoL_1]$	+	MIC	-	-	-	-	-	-	+	MIC	-	-	-	-	-	-
$[NiL_1]$	+	MIC	-	-	-	-	-	-	+	+	+	MIC	-	-	-	-
Fluconazole	+	+	+	MIC	-	-	-	-	+	+	+	+	MIC	-	-	-

Table 5. (Continued)

Where: (+): Growth, (MIC):99%,(-): No growth

3.7. Molecular docking

The results obtained from molecular docking and structural analyses indicate that the primary interactions of the compounds with the Cyclin-dependent kinase 2 (CDK2) protein are concentrated around the amino acids Asp145 and Lys33. These residues form stable interaction bonds with the ligands at the protein's active site. Images show that distances between the ligand and these amino acids range from approximately to 2.8 to 3.0 260 Å, suggesting the presence of hydrogen bonds or polar interactions that likely contribute to stabilizing the ligand within the active site. These critical interactions highlight the importance of targeting Asp145 and Lys33 as key sites for drug design, as focusing on these residues can enhance the efficacy and selectivity of the designed compounds. The understanding of these interactions provides information about ligand binding and stability mechanism, which can be leveraged in order to create molecules that are more potent with improved therapeutic properties through techniques of the structural designs. In addition to that, this analysis emphasizes the necessity to explore the specific targeting of those sites to develop compounds interacting more selectively with Asp-145 and Lys-33, which results in the increase of therapeutic effectiveness and the reduction of any unwanted side effects. The findings represent one of the essential steps towards the rational design of new drugs that precisely target (CDK2)^[35]. As shown in (Figure 4, Figure 5, Table 6).

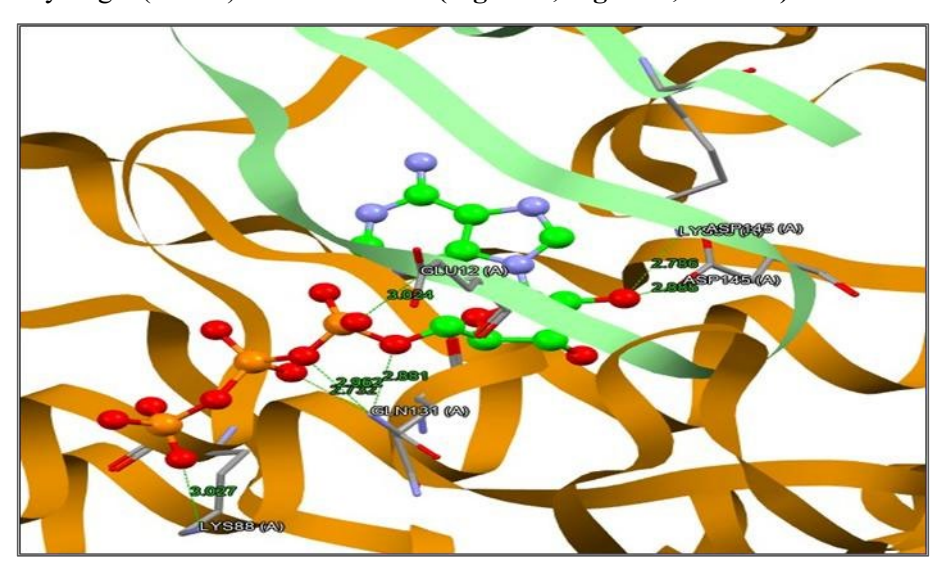


Figure 4. Three-dimensional structure of CDK2.

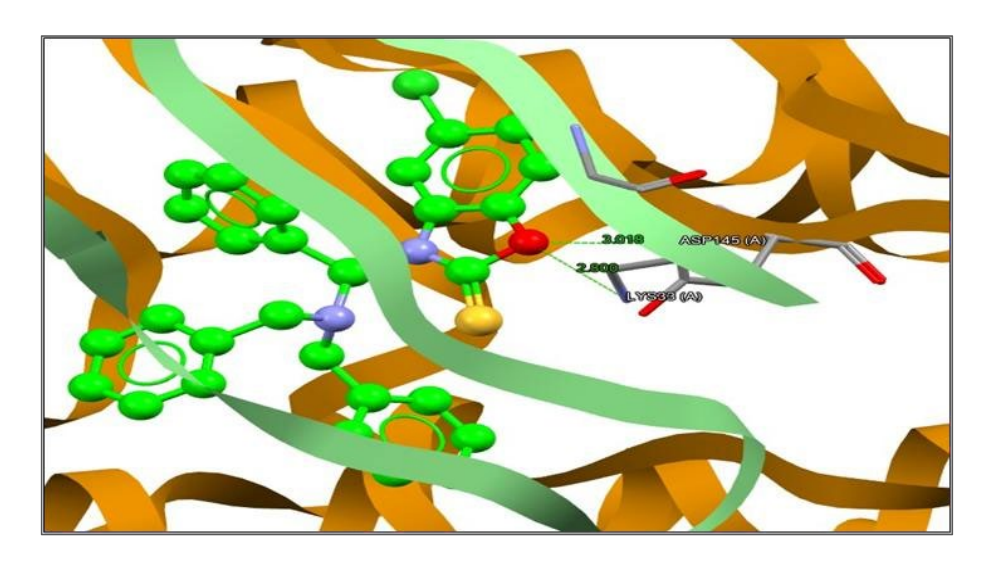


Figure 5. Molecular docking interactions of the ligand with the active site of CDK2, highlighting interactions with residues Asp145 and Lys33.

Table 6. Distances and interactions between the ligand and key active site residues of CDK2, specifically Asp145 and Lys33.

Docking study											
Comp.	Binding Energy (PLP Fitness) Kcal/Mol	No. of H-bonding Included in Amino Acids	Amino Acids Included in H-bonding	no. of bonding	power of bonding						
			GLU 12	1	3.024						
			LYS 33	1	2.786						
			LYS 88	1	3.027						
1HCK	60.41	7			2.732						
			GLN 131	3	2.881						
					2.962						
			ASP 145	1	2.885						
Ι.	60.54	2	LYS 33	1	2.8						
L_1	60.54	2	ASP 145	1	3.018						

4. Conclusion

Metal The spectroscopic and analytical data verified that the ions Cr(III), Mn(II), Co(II), and Ni(II) were successfully coordinated with the Mannich base ligand. The molar conductance values showed that the complexes were not electrolytic, even though the electronic spectra and magnetic moment measurements agreed with octahedral geometries for the Cr(III), Mn(II), and Ni(II) complexes, and a tetrahedral geometry for the Co(II) complex. The complexes' electrical configuration and coordination environment may change, as suggested by these structural assignments, which may have an impact on their biological function. The Co(II) and Ni(II) complexes shown the best inhibitory effects against Gram-positive (*S.aureus*) and Gram-negative (*E. coli*) bacteria, as well as fungal strains (*A. flavus* and *Penicillium spp.*), according to the antimicrobial data (**Table 5**). The Cr(III) complex, on the other hand, had the least antibacterial action, while the Mn(II) complex shown rather moderate activity. The Co(II) tetrahedral complex and the Ni(II) octahedral complex offer more advantageous interactions with microbial targets, perhaps increasing their bioavailability and binding affinity. These variations in stability and geometry may be the cause of this variance in activity. Importantly, the ligand by itself also demonstrated antibacterial activity, but the presence of metal ions significantly boosted its efficacy. The reported structure–activity relationship suggests that the nature of the core metal ion and its

coordination environment play a key role in controlling biological activity. These results are further supported by molecular docking tests, which confirmed the ligand's strong binding affinities with biological macro molecules. Overall, the comparative analysis shows that the most promising candidates for therapeutic applications are Co(II) and Ni(II) complexes. The findings also indicate the advantageous role that metal complexation plays in boosting the antibacterial capabilities of the Mannish base ligand.

Acknowledgments

The authors are grateful to the department of chemistry at the college of science at Al Mustansiriyah university for providing the facilities and constant encouragement for this work.

Conflict of interest

The authors declare no conflict of interest.

References

- 1. Smith J., Petrovic P., Rose M., De Souz C., Muller L., Nowak B., Martinez J., Placeholder Text: A Study, The Journal of Citation Styles, 2021, 3:2000
- 2. Tamilvendan D., Rajeswari S., Ilavenil S., Chakkaravarthy K., Venkatesa Prabhu G., Syntheses, spectral, crystallographic, antimicrobial, and antioxidant studies of few Mannich bases, Medicinal Chemistry Research, 2012, 21:4129
- 3. Kalia S., Jasrotia R., Singh V.P. (eds.). Magnetic Nanoferrites and Their Composites: Environmental and Biomedical Applications. Elsevier; 2023.
- 4. Afsah E.M., Elmorsy S.S., Abdelmageed S.M., Zaki Z.E., Synthesis of some new mixed azines, Schiff and Mannich bases of pharmaceutical interest related to isatin, Zeitschrift für Naturforschung B, 2015, 70:393
- 5. Biersack B., Ahmed K., Padhye S., Schobert R., Recent developments concerning the application of the Mannich reaction for drug design, Expert Opinion on Drug Discovery, 2018,13:39
- 6. Waheed E.J., Al-Khazraji A., Ahmed A.A., Versatile applications of mannich base ligands and their metal complexes: a review article, Journal of Applied Sciences and Nanotechnology, 2023,3:42
- 7. Khazaal A.Q., Mahmood Z.F., Hammood S.A., Analyzing the characteristics and biological activities of methanolic extracts from Stachys byzantina leaves, Iraqi Journal of Agricultural Sciences, 2024, 55:1894
- 8. Etheb A.M., Al-Jeboori M.J., Synthesis, structural characterisation and biological activity of new Mannich compounds derived from cyclohexanone moiety, HIV Nursing, 2022, 22:3659
- 9. Saleh H.A., Abdul Rahman A.S.A., Al-Jeboori M.J., Synthesis, structural characterisation and biological evaluation of new semicarbazone metal complexes derived from Mannich-base, Biochemical & Cellular Archives, 2021, 21:1
- 10. Subrahmanian S., Thirumoorthy K., Singh R.R., Prasad M., Mannich metal complex: Synthesis, reaction mechanism and computational studies, Journal of Molecular Structure, 2022, 1268:133625.
- 11. Manhee T.Q., Alabdali A.J., Synthesis, characterization, and anticancer activity of Ni(II), Cu(II), Pd(II), and Au(III) complexes derived from a novel Mannich base, Vietnam Journal of Chemistry, 2024, 62:201.
- 12. Aldeen S.W.A., Abbass N.M., Metal complexes of Metronidazole Benzoate with some metal ions: synthesis and characterization and study apart from their biological applications,2023.
- 13. Kadhim H.M., Kadhim Y.M., Fawzi H.A., Abdul Khalik Z.M., Jawad A.M., Ghédira K., Bioassay-guided isolation and active compounds identification of the antidiabetic fractions of Centaurea calcitrapa extract and the predicted interaction mechanism, Molecules, 2025, 30:2394.
- 14. Shimanouchi T., Matsuura H., Ogawa Y., Harada I., Tables of molecular vibrational frequencies, Journal of Physical and Chemical Reference Data, 1978, 7:1323.
- 15. Karaağaç D., Spectroscopic and thermal studies of cyano bridged hetero-metallic polymeric complexes derived from ligands containing N and S donor atoms, Bulletin of the Chemical Society of Ethiopia, 2020, 34:365.
- 16. Koucký F., Dobrovolná T., Kotek J., Císařová I., Havlíčková J., Liška A., Hermann P., Transition metal complexes of the (2,2,2-trifluoroethyl) phosphinate NOTA analogue as potential contrast agents for 19F magnetic resonance imaging, Dalton Transactions, 2024, 53:9267.
- 17. Al-Jeboori M.J., New metal complexes derived from Mannich-base ligand: synthesis, spectral characterisation and biological activity, J. Global Pharma Tech, 2019, 11:548.
- 18. Al-Fakeh M.S., Alsikhan M.A., Alnawmasi J.S., Physico-chemical study of Mn(II), Co(II), Cu(II), Cr(III), and Pd(II) complexes with Schiff-base and aminopyrimidyl derivatives and anti-cancer, antioxidant, antimicrobial applications, Molecules, 2023, 28:2555.
- 19. Bartyzel A., Synthesis, thermal study and some properties of N2O4–donor Schiff base and its Mn(III), Co(II), Ni(II), Cu(II) and Zn(II) complexes, Journal of Thermal Analysis and Calorimetry, 2017, 127:2133.

- 20. Dai F., Zhuang Q., Huang G., Deng H., Zhang X., Infrared spectrum characteristics and quantification of OH groups in coal, ACS Omega, 2023, 8:17064.
- 21. Al-Fakeh M.S., Alsikhan M.A., Alnawmasi J.S., Alluhayb A.H., Al-Wahibi M.S., New nanosized V(III), Fe(III), and Ni(II) complexes comprising Schiff base and 2-amino-4-methyl pyrimidine: synthesis, properties, and biological activity, International Journal of Biomaterials, 2024, 2024:9198129.
- Kalinin A.A., Yusupova G.G., Burganov T.I., Dudkina Y.B., Islamova L.N., Levitskaya A.I., Balakina M.Y., Isomeric indolizine-based π-expanded push–pull NLO-chromophores: synthesis and comparative study, Journal of Molecular Structure, 2018, 1156:74.
- 23. Alya'a J.A., Alias M.F., Anticancer, antioxidant and antimicrobial evaluation of Cr(III) and Rh(III) complexes derived from a new Mannich base, Iraqi Journal of Science, 2024, 4853.
- 24. Al-Khazraji A.M., Al Hassani R.A., Ahmed A., Studies on the photostability of polystyrene films with new metals complex of 1,2,4-triazole-3-thione derivate, Sys Rev Pharm, 2020, 11:525.
- 25. Taylor L.J., Kays D.L., Low-coordinate first-row transition metal complexes in catalysis and small molecule activation, Dalton Transactions, 2019, 48:12365
- 26. Cini R., Cinquantini A., Seeber R., Complexes of magnesium(II) and other divalent metal ions with adenosine 5-triphosphate and 2,2-dipyridylamine in aqueous solution, Inorganica Chimica Acta, 1986, 123:69.
- 27. Abdel-Rahman L.H., Abdelghani A.A.A., AlObaid A.A., El-ezz D.A., Warad I., Shehata M.R., Abdalla E.M., Novel bromo and methoxy substituted Schiff base complexes of Mn(II), Fe(III), and Cr(III) for anticancer, antimicrobial, docking, and ADMET studies, Scientific Reports, 2023, 13:3199.
- 28. Rasheed A.M., Al-Bayati S.M., Al-Hasani R.A., Shakir M.A., Synthesizing, structuring, and characterizing bioactivities of Cr(III), La(III), and Ce(III) complexes with nitrogen, oxygen, and sulfur donor bidentate Schiff base ligands, Baghdad Science Journal, 2021, 18:1545
- 29. Barad S., Saurabh S., Choquesillo-Lazarte D., Jadeja R.N., Chemical assessment of three octahedral Ni(II) complexes with heterocyclic acylpyrazolone ligand: crystal structure, DFT-NBO analysis, Hirshfeld and magnetic study, Journal of Molecular Structure, 2025, 1321:140213.
- 30. Burger K., Millar I.T., Allen D.W., Bogyo G., Coordination chemistry: experimental methods, 1973.
- 31. Hassan S.S., Mohamed E.F., Maged K., Hassan S., Hamad A.O., Nasr S., Saleh A.M., Synthesis of new Cu(II), Ni(II), and Cd(II)-(N-Glycyl-L-leucine) complexes as peptide metalloantibiotics for targeting pathogenic water with antioxidant effect investigation, Beni-Suef University Journal of Basic and Applied Sciences, 2025, 14:1.
- 32. Abu-Dief A.M., Shehata M.R., Hassan A.E., Alharbi S.K., Alzahrani A.Y.A., Abo-Dief H.M., Ragab M.S., Exploring anthranilic azomethine complexes: from synthesis, spectroscopic, solution and theoretical studies to DNA interaction and biomedical prospects, Journal of Molecular Structure, 2025, 142571.
- 33. Besleaga I., Raptová R., Stoica A.C., Milunovic M.N., Zalibera M., Bai R., Arion V.B., Are the metal identity and stoichiometry of metal complexes important for colchicine site binding and inhibition of tubulin polymerization?, Dalton Transactions, 2024, 53:12349
- 34. Zhang H.Z., Zhao Z.L., Zhou C.H., Recent advance in oxazole-based medicinal chemistry, European Journal of Medicinal Chemistry, 2018, 144:444.
- 35. Schulze-Gahmen U., De Bondt H.L., Kim S.H., High-resolution crystal structures of human cyclin-dependent kinase 2 with and without ATP: bound waters and natural ligand as guides for inhibitor design, Journal of Medicinal Chemistry, 1996, 39:4540.